Energies and Auger widths of the high-lying triply excited states for Li-like beryllium

BingCong Gou, JingJing Zhu, and Yan Sun
Department of Physics, Beijing Institute of Technology, Beijing 100081, People's Republic of China
(Received 16 September 2009; published 11 December 2009)

The energies, fine-structure splittings, Auger channel energies, and the Auger widths of the high-lying triply excited $2l2l'nl''$ $(n \geq 2)$ states of ^2S, ^2D, and $^2P^o$ resonances for Be^+ are studied using the saddle-point variational method and saddle-point complex-rotation method. The relativistic corrections and mass polarization are included using the first-order perturbation theory. Restricted variational method is carried out to extrapolate better energies. The partial Auger widths are calculated for the individual open channels and the total Auger widths are obtained by coupling the important open channels and summing over the other channels. The configuration mixings of the triply excited resonances are described and differences in the literature on the designation of the intershell states are pointed out. These results are compared with other theoretical and experimental data in the literature.

DOI: 10.1103/PhysRevA.80.062512 PACS number(s): 32.10.Fn

I. INTRODUCTION

With the development of extreme-ultraviolet synchrotron light sources and detection techniques, the high-quality photoabsorption data on the triply excited atomic system with both 1*s*-shell orbitals vacant have been obtained. The highly excited Li-like atomic system is an ideal system for investigating the electron correlations and for testing theoretical methods in dealing with such problems. In the past few decades, the hollow states of Li-like ions have been the subject of intense experimental [1–6] and theoretical [6–19] interests.

Bruch and co-workers [1,2] first reported the triply excited states of Li-like beryllium in beam-foil experiments. In 1984, Agentoft *et al.* [3] reported the first observation of the decay of the triply excited Be^+ state $2p2p2p\ ^4S^o$ in an optical emission spectrum. The first photoexcitation experiment on hollow lithium was carried out by Kiernan *et al.* [4] who measured the energy and width of the $2s^22p\ ^2P^o$ state. Journel *et al.* [5] made the first partial photoionization cross section measurement in the triply excited energy region. Theoretically, Conneely and Lipsky [9,10] calculated the energies and configuration mixings of the triply excited states of the Li isoelectronic sequence $(Z=3-10)$ using the truncated diagonalization method (TDM). The energies and widths of the triply excited states of Li isoelectronic sequence have also been calculated using the multiconfiguration Hartree-Fock [7] method, the multiconfiguration Dirac-Fock method [8], the saddle-point complex-rotation method [11–13], the *R* matrix [5,14–16], and the density-functional theory (DFT) [17]. So far, most studies have been able to classify intrashell triply excited states, but a few intershell states.

In this work, the high-lying triply excited states $^2S(m)$, $^2D(m)$, and $^2P^o(m)$ $(m=2-7)$ for Be^+ are extended and investigated [12]. The resonance energies and widths are calculated with the saddle-point variational method and saddle-point complex-rotation method. A restricted variational method is used for the saturated wave functions. Relativistic corrections and mass polarization are computed using first-order perturbation theory. The fine structures and Auger channel energies are also reported and discussed.

II. THEORY

In the *LS* coupling scheme, the nonrelativistic Hamiltonian for the Li-like ions is given by (in a.u.)

$$\hat{H}_0 = \sum_{i=1}^{3} \left[-\frac{1}{2}\nabla_i^2 - \frac{Z}{r_i} \right] + \sum_{\substack{i,j=1 \\ i<j}}^{3} \frac{1}{r_{ij}}. \tag{1}$$

In general, the closed-channel wave function of the triply excited three-electron system can be written as

$$\Psi_b(1,2,3) = A[1-P(1)][1-P(2)][1-P(3)]\psi(1,2,3), \tag{2}$$

where A is the antisymmetrization operator. The projection operator P is given by

$$P(i) = |\phi_0(\boldsymbol{r}_i)\rangle\langle\phi_0(\boldsymbol{r}_i)|, \tag{3}$$

where the vacancy orbital is

$$\phi_0(\boldsymbol{r}) = N \exp(-qr). \tag{4}$$

q is the nonlinear parameter determined in the energy maximization process and N is a normalization constant. The radial basis functions in $\psi(1,2,3)$ are Slater orbitals. The linear and nonlinear parameters in $\psi(1,2,3)$ are determined in the energy optimization process. E_b obtained from $\Psi_b(1,2,3)$ is the saddle-point energy of the triply excited state. The total energy is further improved by including the relativistic corrections and mass polarization effect calculated using first-order perturbation theory. The relativistic perturbation operators considered in this work are correction to the kinetic energy (P^4), the Darwin term, the electron-electron contact term, and the orbit-orbit interaction. The explicit expressions for these operators are given in [20], and they will not be repeated here. To saturate the functional space, the restricted variational method [20] is used to further improve the saddle-point energy E_b; the nonrelativistic energy is obtained by adding improvement from the restricted variation ΔE_{RV}.

To obtain the width that comes from the interaction of the closed-channel part with the open channels using the saddle-

TABLE I. Nonrelativistic energies (in a.u.) of triply excited states $^2S(m)$, $^2D(m)$, and $^2P^o(m)$ $(m=2-7)$ for Li-like beryllium. q is the nonlinear parameter in the vacancy orbital.

Resonances	q	E_b	ΔE_{RV}	ΔE_S	E_{nonrel}	
					This work	Others
$2s2s3s\ ^2S(2)$	3.917	−3.8682104	−0.0000798	0.0009965	−3.8672937	−3.861006,[a] −3.8160356 [b]
$2s2p(^3P^o)3p\ ^2S(3)$	3.908	−3.7541679	−0.0000846	0.0009774	−3.7532751	−3.745425 [a]
$2s2s4s\ ^2S(4)$	3.913	−3.7031066	−0.0000812	0.0006729	−3.7025149	−3.695650,[a] −3.6506409 [b]
$2s2p(^3P^o)4p\ ^2S(5)$	3.927	−3.6447324	−0.0000803	0.0093562	−3.6354565	−3.634432 [a]
$2s2p(^3P^o)5p\ ^2S(6)$	3.910	−3.6362267	−0.0000837	0.0005539	−3.6357565	−3.628238 [a]
$2s2p(^1P^o)3p\ ^2S(7)$	3.927	−3.6152002	−0.0000815	0.0005891	−3.6146926	−3.605276 [a]
$2s2p(^3P^o)3p\ ^2D(2)$	3.907	−3.7812067	−0.0000894	0.0006901	−3.7806060	−3.774274 [a]
$2s2s3d\ ^2D(3)$	3.911	−3.7708914	−0.0000928	0.0005284	−3.7704558	−3.763162,[a] −3.7190408 [b]
$2p2p(^1D)3s\ ^2D(4)$	3.905	−3.6707869	−0.0000918	0.0059385	−3.6649402	−3.660749,[a] −3.6401292 [b]
$2s2s4d\ ^2D(5)$	3.910	−3.6659883	−0.0000921	0.0004480	−3.6656324	−3.656298,[a] −3.6158346 [b]
$2s2p(^3P^o)4p\ ^2D(6)$	3.913	−3.6333624	−0.0000887	0.0007154	−3.6327357	−3.628638 [a]
$2s2p(^3P^o)4f\ ^2D(7)$	3.906	−3.6250620	−0.0000876	0.0000329	−3.6251167	−3.618460 [a]
$2p2p2p\ ^2P^o(2)$	3.988	−4.0759554	−0.0001368	0.0028233	−4.0732689	−4.054180 [a]
$2s2s3p\ ^2P^o(3)$	3.910	−3.8409893	−0.0000996	0.0007660	−3.8403229	−3.834417,[a] −3.7752382 [b]
$2s2p(^3P^o)3s\ ^2P^o(4)$	3.901	−3.8004718	−0.0001186	0.0006794	−3.7999110	−3.791523 [a]
$2s2p3d\ ^2P^o(5)$	3.911	−3.7156740	−0.0001161	0.0004352	−3.7153549	−3.708900 [a]
$2s2s4p\ ^2P^o(6)$	3.912	−3.6891326	−0.0000967	0.0008116	−3.6884177	−3.681821,[a] −3.6358289 [b]
$2s2p(^1P^o)3s\ ^2P^o(7)$	3.903	−3.6603372	−0.0001161	0.0005305	−3.6599227	−3.659015 [a]

[a]Reference [10].
[b]Reference [17].

point complex-rotation method, we write the total wave function as

$$\Psi(1,2,3) = \Psi_b(1,2,3) + \sum_i A\phi_i(1,2)U_i(3), \tag{5}$$

where

$$U_i = \sum_n d_{i,n} r^n \exp(-\alpha_i r). \tag{6}$$

Here $\phi_i(1,2)$ represents the two-electron open-channel target state and U_i represents the wave function of the outgoing electron. In the complex-rotation computation, only r in U_i is complex scaled. The energy from $\Psi(1,2,3)$, $E-i\Gamma/2$, gives the position and the width of the resonance. The difference, $\Delta E_s = E - E_b$, represents the shift from the saddle-point energy to the resonance energy due to the interaction between $\Psi_b(1,2,3)$ and continua. Finally, we obtain the energy of the resonance,

$$E_{total} = E_b + \Delta E_{RV} + \Delta E_s + \Delta E_{rel} + \Delta E_{mp}. \tag{7}$$

The fine-structure perturbation operators are given by

$$H_{FS} = H_{SO} + H_{SOO} + H_{SS}, \tag{8}$$

where the spin-orbit, spin-other-orbit, and spin-spin operators are

$$H_{SO} = \frac{Z}{2c^2} \sum_{i=1}^{3} \frac{\boldsymbol{l}_i \cdot \boldsymbol{s}_i}{r_i^3}, \tag{9}$$

$$H_{SOO} = -\frac{1}{2c^2} \sum_{\substack{i,j=1 \\ i \neq j}}^{3} \left[\frac{1}{r_{ij}^3} (\boldsymbol{r}_i - \boldsymbol{r}_j) \times \boldsymbol{P}_i \right] \cdot (\boldsymbol{s}_i + 2\boldsymbol{s}_j), \tag{10}$$

$$H_{SS} = \frac{1}{c^2} \sum_{\substack{i,j=1 \\ i<j}}^{3} \frac{1}{r_{ij}^3} \left[\boldsymbol{s}_i \cdot \boldsymbol{s}_j - \frac{3(\boldsymbol{s}_i \cdot \boldsymbol{r}_{ij})(\boldsymbol{s}_j \cdot \boldsymbol{r}_{ij})}{r_{ij}^2} \right]. \tag{11}$$

One important question in the calculation is how to determine the main configuration of a particular high-lying resonance. In this work, each resonance is identified by three factors: the energy, the relative contribution to normalization of the angular-spin components, and a check of the relativistic perturbation correction. We also studied that the fine-structure splittings change with the angular-spin components of the high-lying triply excited states.

III. RESULT AND DISCUSSION

Triply excited states of Li-like ions are a complex three-electron atomic system in which all the three electrons reside in higher shells leaving the K shell empty, which are often referred to as the hollow states. Many relevant angular-spin components are important for the energies. For each set of orbital angular momenta l_1, l_2, and l_3, there could be several ways to couple this set into the desired total orbital angular momentum. In order to get high-quality wave functions, the number of angular-spin components in the wave functions

TABLE II. Relativistic energies of triply excited states $^2S(m)$, $^2D(m)$, and $^2P^o(m)$ $(m=2-7)$ for Li-like beryllium. H_{mp} is the mass polarization and H_{rel} is the relativistic correction.

Resonances	E_{nonrel} (μa.u.)	Perturbation corr. (μa.u.)		E_{total} (a.u.)	
		$\langle H_{mp}\rangle$	$\langle H_{rel}\rangle$	This work	Others
$2s2s3s\ ^2S(2)$	−3867293.7	−0.96	−857.27	−3.868152	−3.856790,[a] −3.86703 [b]
$2s2p(^3P^o)3p\ ^2S(3)$	−3753275.1	4.75	−658.43	−3.753929	−3.739861 [a]
$2s2s4s\ ^2S(4)$	−3702514.9	0.95	−804.67	−3.703319	−3.693539 [a]
$2s2p(^3P^o)4p\ ^2S(5)$	−3635456.5	3.93	−649.34	−3.636102	−3.624845 [a]
$2s2p(^3P^o)5p\ ^2S(6)$	−3635756.5	0.27	−747.11	−3.636503	−3.593361 [a]
$2s2p(^1P^o)3p\ ^2S(7)$	−3614692.6	0.60	−665.24	−3.615357	−3.519036 [a]
$2s2p(^3P^o)3p\ ^2D(2)$	−3780606.0	10.13	−705.06	−3.781301	
$2s2s3d\ ^2D(3)$	−3770455.8	−3.96	−732.06	−3.771192	
$2p2p(^1D)3s\ ^2D(4)$	−3664940.2	3.74	−558.57	−3.665495	
$2s2s4d\ ^2D(5)$	−3665632.4	−1.72	−738.53	−3.666373	
$2s2p(^3P^o)4p\ ^2D(6)$	−3632735.7	1.58	−620.68	−3.633355	
$2s2p(^3P^o)4f\ ^2D(7)$	−3625116.7	1.27	−598.22	−3.625714	
$2p2p2p\ ^2P^o(2)$	−4073268.9	15.56	−458.81	−4.073712	−4.023284,[a] −4.1046 [c]
$2s2s3p\ ^2P^o(3)$	−3840322.9	−2.91	−777.56	−3.841103	−3.830643 [a]
$2s2p(^3P^o)3s\ ^2P^o(4)$	−3799911.0	0.87	−709.54	−3.800620	−3.786295 [a]
$2s2p3d\ ^2P^o(5)$	−3715354.9	2.83	−638.46	−3.715991	−3.705008 [a]
$2s2s4p\ ^2P^o(6)$	−3688417.7	0.19	−764.95	−3.689182	−3.679182 [a]
$2s2p(^1P^o)3s\ ^2P^o(7)$	−3659922.7	1.95	−621.58	−3.660542	−3.651669 [a]

[a]Reference [21].
[b]Reference [22].
[c]Reference [23].

ranges from 26 to 43, and the number of linear parameters ranges from 763 to 1149. To saturate the wave functional space and to improve the energy E_b obtained from $\Psi_b(1,2,3)$, the restricted variational method is used to compute energy contributions from each chosen angular-spin series.

In Table I, we report the nonrelativistic energies of the high-lying triply excited states $2l2l'nl''$, $^2S(m)$, $^2D(m)$, and $^2P^o(m)$ $(m=2-7)$, for Li-like beryllium. To extend the earlier calculation of Gou and Chung [12], m indicates that the corresponding state is the mth lowest triply excited state. In Table I, q is the nonlinear parameter in the vacancy orbital determined in the energy maximization process and can be roughly interpreted as the effective nuclear charge seen by the $1s$-vacancy orbital. E_b is the energy calculated from the closed-channel wave function. ΔE_{RV} is the total correction to E_b from the restricted variation calculations and ΔE_S is the total-energy shift that comes from the interaction of the closed-channel part with the open channels. The nonrelativistic energy E_{nonrel} is obtained by adding E_b, ΔE_{RV}, and ΔE_S. As Table I shows, for all cases, the nonrelativistic energies in this work are lower than those of Conneely and Lipsky (TDM) [10] and Roy (DFT) [17]. The improvements range from −0.0009 to −0.0191 a.u. and from −0.0248 to −0.0651 a.u., respectively.

Table II presents the relativistic energies of the triply excited states for Be^+. The triply excited intershell states are numbered according to their position in the series; the second lowest is denoted by (2). Each state is approximately identified by the following three factors: the energy, the relative contribution to normalization of the angular-spin components, and a check of the relativistic perturbation correction. We note that a $2s2snl$ state has a larger relativistic perturbation correction than the $2s2pnl$ state, which in turn has a larger correction than that of the $2p2pnl$ state. As Table I shows, for ^2S, the relativistic effect of $2s2s3s\ ^2S(2)$ state, −857.27 μa.u., is apparently larger than that of $2s2p3p\ ^2S(3)$ state, −658.43 μa.u., and $2s2p4p\ ^2S(5)$ state, −649.34 μa.u. For $^2S(6)$, the contribution of spp angular-spin component to the state is 54.52% and sss is 45.13%; the relativistic effect of $^2S(6)$ is −747.11 μa.u., so identifying $2s2p5p$ for $^2S(6)$ will be more reasonable than $2s2s5s$. It is different from the assignment reported by Conneely and Lipsky (TDM) [10]. For the same reason, for ^2D, the relativistic effect of $2p2p3s\ ^2D(4)$ state, −558.57 μa.u., is apparently smaller than that of $2s2p3p\ ^2D(2)$ state, −705.06 μa.u., and $2s2p4p\ ^2D(6)$ state, −620.68 μa.u.; so identifying $2p2p3s$ for $^2D(4)$ will be more reasonable than $2s2p4p$. It is different from the assignment reported by Conneely and Lipsky (TDM) [10].

The relativistic energies given in Table II are the center-of-gravity energies. Including the effects of the spin-orbit, spin-other-orbit, and spin-spin interactions, we obtain the energies of the fine-structure-resolved J levels. Table III gives the shifts of the various J levels from the center-of-gravity energies and the fine-structure splittings of high-lying triply excited states ^2D and $^2P^o$ for Be^+. So far, to our knowledge, no calculations of the fine-structure have been reported for

TABLE III. Center-of-gravity total energies E_{CG}, fine-structure correlations ΔE_J, and fine-structure splittings $\nu_{J-J'}$ of triply excited states $^2D(m)$ and $^2P^o(m)$ $(m=2-7)$ for Li-like beryllium.

Resonances	E_{CG} (a.u.)	ΔE_J (μa.u.)		$\nu_{2.5-1.5}$ (cm^{-1})
		$J=2.5$	$J=1.5$	
$2s2p(^3P^o)3p\ ^2D(2)$	−3.781301	55.25	−82.88	30.31
$2s2s3d\ ^2D(3)$	−3.771192	25.37	−38.06	13.92
$2p2p(^1D)3s\ ^2D(4)$	−3.665495	9.20	−13.80	5.05
$2s2s4d\ ^2D(5)$	−3.666373	1.92	−2.88	1.05
$2s2p(^3P^o)4p\ ^2D(6)$	−3.633355	54.23	−81.35	29.76
$2s2p(^3P^o)4f\ ^2D(7)$	−3.625714	−39.17	58.75	−21.49
		$J=1.5$	$J=0.5$	$\nu_{1.5-0.5}$ (cm^{-1})
$2p2p2p\ ^2P^o(2)$	−4.073712	11.01	−22.02	7.25
$2s2s3p\ ^2P^o(3)$	−3.841103	31.33	−62.67	20.63
$2s2p(^3P^o)3s\ ^2P^o(4)$	−3.800620	50.53	−101.05	33.26
$2s2p3d\ ^2P^o(5)$	−3.715991	−34.91	69.82	−22.99
$2s2s4p\ ^2P^o(6)$	−3.689182	10.06	−20.13	6.63
$2s2p(^1P^o)3s\ ^2P^o(7)$	−3.660542	57.65	−115.30	37.96

the corresponding triply excited states. Figure 1 gives the systematical change in the fine-structure splittings of the triply excited states $^2D(m)$ and $^2P^o(m)$ $(m=2-7)$ along with m increasing for Be^+. In Fig. 1, we note that the drastic change in the fine-structure splittings at $2s2p3d\ ^2P^o(5)$ or $2s2p4p\ ^2D(6)$ is reasonable according to the assignment of configuration structure for this high-m system as mentioned above. For example, the main configuration of $2s2p3d\ ^2P^o(5)$ is *spd*, but the main configuration of $^2P^o(4)$ and $^2P^o(6)$ is *ssp*. The fine-structure splittings rely on the orbital angular momenta, so the mutation of the fine-structure splittings along with the change in the main configuration of the high-lying triply excited states $^2D(m)$ and $^2P^o(m)$ $(m=2-7)$ is reasonable.

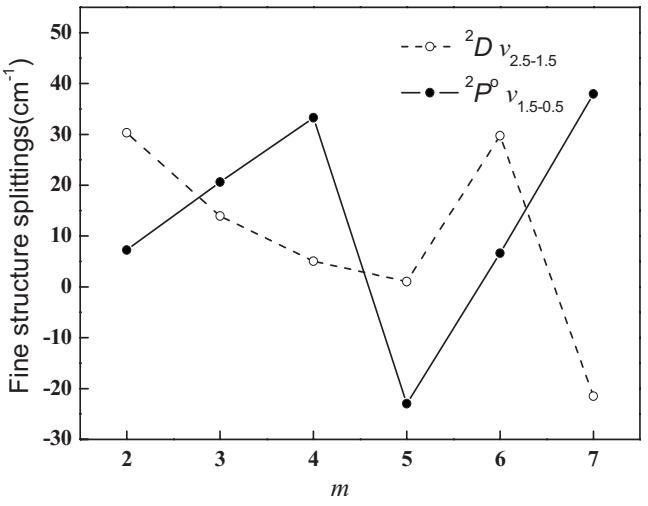

FIG. 1. Fine-structure splittings $\nu_{J-J'}$ (in cm^{-1}) of triply excited states $^2D(m)$ and $^2P^o(m)$ $(m=2-7)$ for Li-like beryllium.

Table IV gives the autoionization channel energies of the triply excited states ^2S, ^2D, and $^2P^o$ for Be^+. These states can decay via many channels. We have calculated only the $1s2s\ ^{1,3}S$, $1s2p\ ^{1,3}P$ Auger channel energies in this work because they are the only Auger channels relevant to the experimental and other theoretical results. To examine the calculation precision for triply excited states, we also list the other theoretical and experimental data. For example, for the $2s2s3s\ ^2S(2)\rightarrow(1s2s^3S+e)$ channel, our calculated energy is 147.738 eV, which agrees well with the experiment of Davis and Chung [22], in which line 52 is reported at 147.763 eV. For the $2p2p2p\ ^2P^o(2)\rightarrow(1s2s^3S+e)$ channel, our calculated energy is 142.063 eV, which agrees well with 142.201 eV reported by Davis and Chung [22] and the experiment of Rødbro *et al.* [2], in which line 48 is reported at 142.4 ± 0.3 eV. For the $2p2p2p\ ^2P^o(2)\rightarrow(1s2p^3P+e)$ channel, our calculated energy is 138.737 eV, which agrees well with the experiment of Rødbro *et al.* [2], in which line 46 is reported at 138.8 ± 0.2 eV, and with the result of Davis and Chung [22] who reported the energy of 138.875 eV. Table IV shows that our results are in good agreement with other theoretical and experimental results.

In Table V, we report the partial widths and total widths of the high-m triply excited states ^2S, ^2D, and $^2P^o$ for Be^+. Triply excited states in Be^+ are located above the third ionization limit, i.e., above the $1s$ ground state of the Be^{3+} ion. So there are an infinite number of open channels associated with each of these triply excited states. We first calculated the partial width for each individual open channel. We then couple all the important open channels and sum over the other channels to calculate the total width Γ and the total shift ΔE_S. Because the Coulomb interaction is a two-particle operator, most of the open channels that differ from the initial $2l2l'nl''$ state by three electronic configurations are expected to have very small contribution to the width. Hence, there are only certain open channels that are important for a particular resonance. The number of important open channels also depends on the symmetry of the resonance. For example, for the lowest $2s2s3s\ ^2S(2)$ state calculated in this work, the main Auger channels according to the branching ratios are

$$2s2s3s\ ^2S\rightarrow 1s3s\ ^3S+ks,\quad 68.25\%$$

$$\rightarrow 1s3s\ ^1S+ks,\quad 15.21\%$$

$$\rightarrow 1s3p\ ^3P+kp,\quad 11.73\%$$

$$\rightarrow 1s2s\ ^3S+ks,\quad 7.93\%$$

$$\rightarrow 1s4s\ ^3S+ks,\quad 2.15\%$$

$$\rightarrow 1s2p\ ^3P+kp,\quad 1.32\%.$$

Here, *ks* and *kp* represent the Auger electron with angular momentum l. The Auger decay process involves the transfer of energy between two excited electrons interacting through the Coulomb potential, in which the one losing energy ends up filling the vacancy in the resonance whereas the other

TABLE IV. Autoionization channel energies of triply excited states $^2S(m)$, $^2D(m)$, and $^2P^o(m)$ ($m=2-7$) for Li-like beryllium.

Resonances	Auger channel energy (eV)			
	$1s2s\ ^3S$	$1s2s\ ^1S$	$1s2p\ ^3P$	$1s2p\ ^1P$
$2s2s3s\ ^2S(2)$	147.738	144.659	144.393	142.820
Ref. [22]	147.763	144.707	144.438	142.691
Ref. [2]			144.0 ± 0.3	
$2s2p(^3P^o)3p\ ^2S(3)$	150.841	147.762	147.496	145.923
$2s2s4s\ ^2S(4)$	152.230	149.152	148.885	147.313
$2s2p(^3P^o)4p\ ^2S(5)$	153.818	150.740	150.473	148.910
$2s2p(^3P^o)5p\ ^2S(6)$	154.050	150.972	150.705	149.132
$2s2p(^1P^o)3p\ ^2S(7)$	154.622	151.544	151.277	149.705
$2s2p(^3P^o)3p\ ^2D(2)$	150.105	147.027	146.760	145.188
$2s2s3d\ ^2D(3)$	150.386	147.307	147.041	145.468
Ref. [6] (expt.)	150.47 ± 0.05	147.36 ± 0.05	147.21 ± 0.05	145.20 ± 0.05
Ref. [6] (theor.)	150.42	147.35	147.09	145.34
$2p2p(^1D)3s\ ^2D(4)$	153.109	150.031	149.764	148.192
$2s2s4d\ ^2D(5)$	153.240	150.162	149.895	148.323
$2s2p(^3P^o)4p\ ^2D(6)$	154.128	151.050	150.783	149.210
$2s2p(^3P^o)4f\ ^2D(7)$	154.354	151.275	151.009	149.436
$2p2p2p\ ^2P^o(2)$	142.063	138.993	138.737	136.987
Ref. [22]	142.201	139.145	138.875	137.128
Ref. [2]	142.4 ± 0.3		138.8 ± 0.2	137.0 ± 0.3
$2s2s3p\ ^2P^o(3)$	148.458	145.387	145.131	143.382
Ref. [6] (expt.)	148.60 ± 0.05	145.40 ± 0.05	145.20 ± 0.05	143.88 ± 0.05
Ref. [6] (theor.)	148.57	145.51	145.24	143.49
Ref. [2]				143.7 ± 0.3
$2s2p(^3P^o)3s\ ^2P^o(4)$	149.560	146.489	146.233	144.484
$2s2p3d\ ^2P^o(5)$	151.867	148.797	148.541	146.791
$2s2s4p\ ^2P^o(6)$	152.590	149.519	149.263	147.514
$2s2p(^1P^o)3s\ ^2P^o(7)$	153.373	150.302	150.046	148.297

receiving the energy may escape from this system. It is clear that this transfer of energy is most likely to occur when the two electrons are interacting strongly and are close in spatial location. For $2s2s3s\ ^2S(2)$ state, the Auger decay arises from the interaction of two $2s$ electrons. After this interaction, one of these two electrons falls into $1s$, and the other is kicked out as an s electron. In this case, the Auger branching ratio of the significant decay channel $1s3s\ ^3S+ks$ is 68.25%. Because the two s electrons are close together, their charge distributions have significant overlap and antiparallel spin. The Auger branching ratio of the decay channel $1s2p\ ^3P+kp$ is only 1.32% due to the required change in angular momentum of the electron from s to p. For the same reason, for the $2s2s3d\ ^3D(3)$ resonance, the major contribution comes from the open channel $1s3d\ ^3D+ks$. As Table V shows, for the $2p2p2p\ ^2P^o(2)$ state, the main Auger channel is $2p2p2p\ ^2P^o(2)\rightarrow(1s2p^3P+kp)$, its partial width is 50.86 meV. In this case, the simplest approximation is assuming that these decay channels arise from the interaction of two $2p$ electrons. The two p electrons are close together; their charge distributions also have significant overlap and antiparallel spin. By Auger widths, we can get the Auger transition rates. Knowledge of the Auger transition rates of triply excited states plays an important role in understanding the stabilization of the states formed in collisions between multiply charged ions with atoms, molecules, and surfaces. The information from Table V is very useful in the study of Auger spectra. It is our hope to provide more reliable theoretical data to stimulate further experimental measurements.

IV. CONCLUSION

In this work, the relativistic energies, fine structures, Auger widths, and Auger channel energies for triply excited states $2l2l'nl''\ ^2S$, ^2D, and $^2P^o$ are studied for Li-like beryllium. The energies obtained in this work are much lower than those of the other theoretical data. The identifications of the energy levels for these series are discussed. The Auger channel energies are in good agreement with other theoretical and experimental data. The main Auger decay channels of the Li-like hollow atom system are also discussed. As far as we know, the theoretical results of the Auger widths and Auger

TABLE V. Partial (Γ_p) and total (Γ_{total}) widths of triply excited states $^2S(m)$, $^2D(m)$, and $^2P^o(m)$ (m=2–7) for Li-like beryllium.

Resonances	Γ_p (meV)											Γ_{total} (meV)
	$1s2s\ ^3S/^1S$	$1s2p\ ^3P/^1P$	$1s3s\ ^3S/^1S$	$1s3p\ ^3P/^1P$	$1s4s\ ^3S/^1S$	$1s4p\ ^3P/^1P$	$1s5s\ ^3S/^1S$	$1s5p\ ^3P/^1P$	$1s3d\ ^3D/^1D$	$1s4d\ ^3D/^1D$	$1s5d\ ^3D/^1D$	
$2s2s3s\ ^2S(2)$	12.64/0.36	2.11/0.08	108.81/24.24	18.70/0.11	3.43/0.38		0.22/0.00					159.42
$2s2p(^3P^o)3p\ ^2S(3)$	4.85/0.21	5.29/1.58	0.37/0.14	0.29/8.03	1.97/0.45	0.71/0.81	0.01/0.00	0.06/0.02	0.06/0.02			25.35
$2s2s4s\ ^2S(4)$	4.54/0.19	1.02/0.45	0.49/0.01	2.09/0.99	101.18/35.57	0.11/0.00	13.39/4.74		0.65/0.22			163.21
$2s2p(^3P^o)4p\ ^2S(5)$	0.21/0.47	1.77/3.97	1.87/0.38	14.47/6.27	0.15/0.03	1.92/1.78	22.67/4.91	0.18/0.52	4.39/1.34	0.34/0.03	0.03/0.00	79.51
$2s2p(^3P^o)5p\ ^2S(6)$	4.18/0.16	0.21/0.10	0.00/0.05	0.27/0.00	4.94/0.44	0.64/1.78	57.38/12.35	0.35/0.91	0.16/0.05			71.57
$2s2p(^1P^o)3p\ ^2S(7)$	1.16/0.58	0.14/1.54	3.56/0.78	17.03/3.43	3.26/1.23	0.54/1.25	1.45/1.33	0.92/1.12	6.18/2.05	0.86/0.19	0.04/0.00	48.79
$2s2p(^3P^o)3p\ ^2D(2)$	5.53/0.28	2.39/1.57	1.89/0.25	0.04/5.93	0.02/0.00	0.15/0.16			37.11/12.15	4.81/1.56	0.10/0.00	73.99
$2s2s3d\ ^2D(3)$	8.72/0.23	2.54/0.39	0.60/0.07	1.18/1.54	0.01/0.00	0.15/0.17		0.02/0.00	67.23/21.97	13.49/4.43	0.27/0.08	124.86
$2p2p(^1D)3s\ ^2D(4)$	0.02/0.03	0.69/1.39	45.14/10.25	8.97/1.92	1.76/0.25	0.91/1.00	0.20/0.00			10.35/4.02	5.78/1.76	96.32
$2s2s4d\ ^2D(5)$	0.52/0.01	0.06/0.13	14.54/2.79	0.53/0.11	0.54/0.00	0.27/0.07	0.05/0.00		8.24/2.24	62.61/20.11	39.32/12.68	170.89
$2s2p(^3P^o)4p\ ^2D(6)$	5.19/0.45	5.01/0.34	17.21/4.03	1.45/0.00	0.89/0.04	0.62/4.18	0.20/0.09	0.35/1.72	0.19/0.16	0.03/0.00	0.25/0.09	43.52
$2s2p(^3P^o)4f\ ^2D(7)$	0.13/0.02	0.15/0.08	0.88/0.19	0.14/0.16	0.09/0.00	0.00/0.09	0.01/0.00		0.01/0.00			1.99
$2p2p2p\ ^2P^o(2)$	0.53/0.21	50.86/16.38	0.00/0.12	0.15/0.02		0.01/0.00			0.09/0.41	0.01/0.08		68.26
$2s2s3p\ ^2P^o(3)$	0.15/0.10	9.38/3.83	2.02/0.25	82.74/27.20		2.91/0.52		0.15/0.02	0.36/0.33			129.64
$2s2p(^3P^o)3s\ ^2P^o(4)$	3.76/0.94	10.12/2.30	1.30/2.92	30.71/11.24	0.17/0.14	4.52/1.01						70.18
$2s2p3d\ ^2P^o(5)$		2.35/0.78	0.24/0.00	0.00/0.02	0.02/0.09				2.19/4.78	0.51/1.01		9.61
$2s2s4p\ ^2P^o(6)$	0.04/0.21	0.06/0.03	3.17/1.39	0.91/0.11	0.15/0.34	87.66/30.83	0.01/0.00	16.51/4.02	0.26/0.02			156.81
$2s2p(^1P^o)3s\ ^2P^o(7)$	0.18/0.12	14.18/4.02	2.80/1.08	0.52/0.23	2.14/4.19	1.79/0.83	0.21/0.00	4.69/1.31	0.09/0.02	0.03/0.01		36.50

branching ratios of the hollow ^2S, ^2D, and $^2P^o$ resonances for Li-like beryllium in this work have no experimental and theoretical data in the literature to compare with at present. These available theoretical data should be useful for studying the observed spectrum in future experiments.

ACKNOWLEDGMENTS

The authors are grateful to Dr. Kong T. Chung for his computer code. This work was supported by the National Natural Science Foundation of China under Grant No. 10674015.

[1] R. Bruch, G. Paul, J. Andrä, and L. Lipsky, Phys. Rev. A **12**, 1808 (1975).
[2] M. Rødbro, R. Bruch, and P. Bisgaard, J. Phys. B **12**, 2413 (1979).
[3] M. Agentoft, T. Andersen, and K. T. Chung, J. Phys. B **17**, L433 (1984).
[4] L. M. Kiernan, E. T. Kennedy, J.-P. Mosnier, J. T. Costello, and B. F. Sonntag, Phys. Rev. Lett. **72**, 2359 (1994).
[5] L. Journel, D. Cubaynes, J.-M. Bizau, S. Al Moussalami, B. Rouvellou, F. J. Wuilleumier, L. VoKy, P. Faucher, and A. Hibbert, Phys. Rev. Lett. **76**, 30 (1996).
[6] R. Bruch, H. Merabet, and K. T. Chung, Nucl. Instrum. Methods Phys. Res. B **205**, 488 (2003).
[7] N. A. Piangos and C. A. Nicolaides, Phys. Rev. A **48**, 4142 (1993).
[8] Y. Azuma, S. Hasegawa, F. Koike, G. Kutluk, T. Nagata, E. Shigemasa, A. Yagishita, and I. A. Sellin, Phys. Rev. Lett. **74**, 3768 (1995).
[9] M. J. Conneely and L. Lipsky, At. Data Nucl. Data Tables **86**, 35 (2004).
[10] M. J. Conneely and L. Lipsky, At. Data Nucl. Data Tables **82**, 115 (2002).
[11] K. T. Chung and B. C. Gou, Phys. Rev. A **52**, 3669 (1995).
[12] B. C. Gou and K. T. Chung, J. Phys. B **29**, 6103 (1996).
[13] Y. Zhang and K. T. Chung, Phys. Rev. A **58**, 1098 (1998).
[14] S. Diehl *et al.*, Phys. Rev. Lett. **79**, 1241 (1997).
[15] S. Diehl *et al.*, J. Phys. B **30**, L595 (1997).
[16] K. Berrington and S. Nakazaki, J. Phys. B **31**, 313 (1998).
[17] A. K. Roy, J. Phys. B **38**, 1591 (2005).
[18] T. I. Morishita and C. D. Lin, Phys. Rev. A **57**, 4268 (1998).
[19] T. I. Morishita and C. D. Lin, Phys. Rev. A **59**, 1835 (1999).
[20] J. J. Zhu, B. C. Gou, and Y. D. Wang, J. Phys. B **41**, 065702 (2008).
[21] M. Ahmed and L. Lipsky, Phys. Rev. A **12**, 1176 (1975).
[22] B. F. Davis and K. T. Chung, J. Phys. B **15**, 3113 (1982).
[23] Z. Zhou and Shih-I Chu, Phys. Rev. A **71**, 022513 (2005).